Low-Temperature FTIR Study of Multiple K Intermediates in the Photocycles of Bacteriorhodopsin and Xanthorhodopsin

Andrei K. Dioumaev,* Jennifer M. Wang, and Janos K. Lanyi

Department of Physiology & Biophysics, University of California, Irvine, California 92697

Received: September 8, 2009; Revised Manuscript Received: December 4, 2009

Low-temperature FTIR spectroscopy of bacteriorhodopsin and xanthorhodopsin was used to elucidate the number of K-like bathochromic states, their sequence, and their contributions to the photoequilibrium mixtures created by illumination at 80−180 K. We conclude that in bacteriorhodopsin the photocycle includes three distinct K-like states in the sequence $bR \xrightarrow{h\nu} I^* \rightarrow J \rightarrow K_0 \rightarrow K_E \rightarrow K_L \rightarrow L \rightarrow ...$, and similarly in xanthorhodopsin.

K_0 is the main fraction in the mixture at 77 K that is formed from J. K_0 becomes thermally unstable above ~50 K in both proteins. At 77 K, both J-to-K_0 and K_0-to-K_E transitions occur and, contrarily to long-standing belief, cryogenic trapping at 77 K does not produce a pure K state but a mixture of the two states, K_0 and K_E, with contributions from K_E of ~15 and ~10% in the two retinal proteins, respectively. Raising the temperature leads to increasing conversion of K_0 to K_E, and the two states coexist (without contamination from non-K-like states) in the 80−140 K range in bacteriorhodopsin, and in the 80−190 K range in xanthorhodopsin. Temperature perturbation experiments in these regions of coexistence revealed that, in spite of the observation of apparently stable mixtures of K_0 and K_E, the two states are not in thermally controlled equilibrium. The K_0-to-K_E transition is unidirectional, and the partial transformation to K_E is due to distributed kinetics, which governs the photocycle dynamics at temperatures below ~245 K (Dioumaev and Lanyi, *Biochemistry* **2008**, *47*, 11125−11133). From spectral deconvolution, we conclude that the K_E state, which is increasingly present at higher temperatures, is the same intermediate that is detected by time-resolved FTIR prior to its decay, on a time scale of hundreds of nanoseconds at ambient temperature (Dioumaev and Braiman, *J. Phys. Chem. B* **1997**, *101*, 1655−1662), into the K_L state. We were unable to trap the latter separately from K_E at low temperature, due to the slow distributed kinetics and the increasingly faster overlapping formation of the L state. Formation of the two consecutive K-like states in both proteins is accompanied by distortion of *two different* weakly bound water molecules: one in K_0, the other in K_E. The first, well-documented in bacteriorhodopsin at 77 K where K_0 dominates, was assigned to water 401 in bacteriorhodopsin. The other water molecule, whose participation has not been described previously, is disturbed on the next step of the photocycle, in K_E, in both proteins. In bacteriorhodopsin, the most likely candidate is water 407. However, unlike bacteriorhodopsin, the crystal structure of xanthorhodopsin lacks homologous weakly bound water molecules.

Introduction

Retinal proteins constitute a rapidly expanding family[1–4] of mostly microbial proteins that can use light for either energy (pumps)[5] or signaling (sensors).[6] Upon absorption of quanta in the visible region, they undergo a cycle of internal transformations that include several obligatory steps. Using the notation H to O to describe the consecutive intermediates first introduced for bacteriorhodopsin,[7,8] these steps include: (i) the initial photophysics (the excited states of H* and I*) where the energy of the absorbed quantum is within the chromophore; (ii) the primary photochemistry (the J and the K-like states) when the retinal is isomerized and the protein begins to readjust to accommodate the new chromophore configuration as the energy is transferred from the chromophore into its immediate environment; and (iii) further steps in which the excess energy stored in the chromophore is fully transferred into the protein. The last phase will depend on the specific function of the protein, but the first two seem to be of general validity, and the sequence of the K-like states covers an important stage in the energetics of the photochemical cycle.

The red-shifted primary intermediates are a general feature in the light-induced photocycles of retinal proteins. In bacteriorhodopsin, as earlier in the visual pigment, a bathochromic state was trapped at 77 K,[9,10] and called K according to the notation proposed in ref 7. When its predecessor was discovered by picosecond spectroscopy,[11] it was called J.[8] Unlike K, the J state cannot be trapped even at 77 K.[12] In the visible region, both J and K states are bathochromic, J being more strongly red-shifted than K.[11,13]

The K state(s) is not a single intermediate[14–16] but rather a generic term for a sequence of spectrally similar species, which at room temperature span the time domain from ~10^{-11} to ~10^{-6} s. The existence of more than one K-like intermediate is supported by evidence from the variety of experimental methods: in visible,[14,16–20] UV,[21] and FTIR spectroscopy,[15,22–28] resonance Raman,[29–31] CARS,[32] and photoelectric measurements.[33] The necessity for more than one K-like intermediate has been evident since the early 1980s.[14,15] However, the question on their number has not been settled, and most authors

* To whom correspondence should be addressed. Phone: (949) 824-7783. Fax: (949) 824-8540. E-mail: dioumaev@uci.edu.

restrict their discussions to the possibility of *two* different K-like states.[14–18,21–31] However, two K-like states are not enough to account for the changes during the early stages of the photocycle, and the pair of K-like intermediates described by time-resolved[24–28] FTIR spectroscopy cannot be the same as the pair of intermediates characterized by low-temperature FTIR.[15,34] Instead, the similarities in the IR spectra between the "high-temperature" state,[15] i.e., the "later" one of the two K states revealed by cryogenic trapping, and the "early K" state[28] described by time-resolved data indicate that *three* different K-like intermediates appear in sequence in the bacteriorhodopsin photocycle between the J and L intermediates.

The vibrational spectra of the K-like state(s) have been studied in detail, by resonance Raman,[29,30,35–39] CARS,[32,40] and IR methods,[15,23,41–45] using static (i.e., trapped at cryogenic temperature)[15,35,41–44,46–48] and time-resolved[23–30,36–40,45] techniques. Detailed assignment of individual vibrational modes was through extensive use of isotope-labeled retinal incorporated into bacteriorhodopsin by Raman[49] (and most fully summarized in ref 50) and by FTIR[44,46,51] methods, creating the basis for studies of other retinal proteins. Both in bacteriorhodopsin[35,41,42] and the other microbial rhodopsins,[52–60] the spectra revealed a well-defined pattern of intensities in the region of hydrogen-out-of-plane (HOOP) vibrations. The HOOP bands are typical for the K-like states, as the other intermediates in the photocycle, with a notable exception of the O state,[61] give rise to little if any intensity in this region.[62] This makes them a convenient feature for monitoring K-like states in microbial rhodopsins. While the early bathochromic intermediates are common to all microbial rhodopsins, their spectra, and especially the pattern of their HOOP bands, vary strongly.[52–60] It was proposed that retinal proteins with sensor and pump function could be distinguished by their HOOP band patterns.[63] We argue here that at least part of the variability in the HOOP of different retinal proteins[52–60] is due to the presence of multiple different K intermediates.

We find that the IR spectra of the K-like states in xanthorhodopsin (a proton-pumping retinal protein/carotenoid complex from *Salinibacter ruber*[64]) are surprisingly similar to those in bacteriorhodopsin, much more so than for other microbial rhodopsins.[52–60] Specifically, the HOOP region, where the temperature-dependent differences between different K-like states were initially found,[15] is very similar in the two proteins. However, unlike in bacteriorhodopsin where L formation interferes with monitoring of K above ~140 K,[48] in xanthorhodopsin, the temperature region where only K-like states are present is extended to ~190 K. This allows a greater extent of temperature-induced transformation and thereby facilitates spectral deconvolution. We found that the interconversions between K-like states is governed by distributed kinetics, which effectively inhibits complete conversions between the states,[48,65] and the extended temperature range in xanthorhodopsin created an opportunity, which we exploited for studying the multiple K-like states.

Experimental Methods

Purple membranes containing wild-type bacteriorhodopsin were isolated according to a standard procedure.[66] The membrane fraction of xanthorhodopsin was isolated as in refs 64 and 67. The samples used were at pH 7.0 and 8–8.5 (1 mM HEPES buffer) for bacteriorhodopsin and xanthorhodopsin, respectively.

Sample preparations and FTIR measurements were as described previously.[48,65,68] In short, infrared measurements were

performed at 2 cm^{-1} resolution on a Bruker IFS-66/s Fourier-transform infrared (FTIR) spectrometer on humidified films of the membrane fragments of xanthorhodopsin and bacteriorhodopsin containing >600 water molecules per molecule of the protein.[68] Low temperature was provided by the Optistat DM cryostat equipped with the ITC601 temperature controller (both from Oxford Instruments, Abingdon, U.K.). Temperature equilibration required ~80 min, after which the cryostat system provided temperature stability within 0.1 K for >5 h. Prior to any measurements, the samples were light-adapted at 280 K for 20 min with a lamp equipped with a 500 ± 20 nm interference filter (referred to as "blue light"). Spectra of intermediates were measured as differences in the IR absorption before and after illumination with blue light, coadding of 1119 interferograms for each spectrum during a 10 min data collection time. Between any pair (of measurements, before and after illumination), the sample temperature was raised to 280 K to complete the photocycle and restore the initial state.

The spectra were interactively corrected for water vapor and, where needed, for baseline distortions. For comparison of spectra measured in separate experiments, the bacteriorhodopsin and xanthorhodopsin spectra were normalized at 1254 and 1253 cm^{-1}, respectively. When a series of spectra trapped at different temperatures required simultaneous analysis, singular value decomposition (SVD) was used. SVD, a matrix algorithm, allows separation of systematic features from stochastic noise,[69] and effectively averages the spectral data over all measured spectra. It improves, therefore, the extraction of spectra of the pure forms from their mixtures.

While IR spectroscopy allows direct monitoring of the overall amount of water in the sample containing retinal proteins,[68] it is not capable of monitoring the distribution of water molecules throughout the sample. Humidity does affect the mixtures trapped at cryogenic temperatures. The main effect observed in the IR is from the contaminating presence of the 13-*cis*,15-*syn* retinal in nonexcited samples (data not shown), which is due to incomplete light adaptation under low humidity.[70] The latter gives rise to a red-shifted photoproduct, different from the K-like states produced from all-*trans* retinal, and in IR, the most affected bands are in the amide, ethylenic stretch, and fingerprint regions.[71,72] No HOOP bands are seen upon light adaptation,[42,71] but there are conflicting reports on whether the HOOP bands are present in the low-temperature photoproduct(s) of the 13-*cis*,15-*syn* retinal at 77 K.[71,72] Our measurements on bacteriorhodopsin samples of different humidity in the 80−140 K range produced spectra, which do differ in the ethylenic and fingerprint regions, reflecting incomplete light adaptation and participation of the 13-*cis*,15-*syn* chromophore. However, the presence of the photoproduct(s) of the 13-*cis*,15-*syn* retinal fails, in accord with the 77 K data of the Rothschild group,[71] to affect the HOOP region (our unpublished data). Since the conclusions in this paper are primarily based on the analysis of the HOOP band region, we believe that they are, therefore, free from the potentially disturbing influence of limited hydration and potentially incomplete light adaptation.

OPUS (Bruker, Germany), GRAMS (Galactic Industries Corp., Salem, NH), Matlab (The MathWorks Inc., Natick, MA), and KaleidaGraph (Synergy Software, Reading, PA) software were used for data evaluation and presentation.

Results

IR spectra obtained at 80 K after 10 min illumination with blue light (500 ± 20 nm) of bacteriorhodopsin and xanthorhodopsin films equilibrated with H$_2$O and D$_2$O are presented
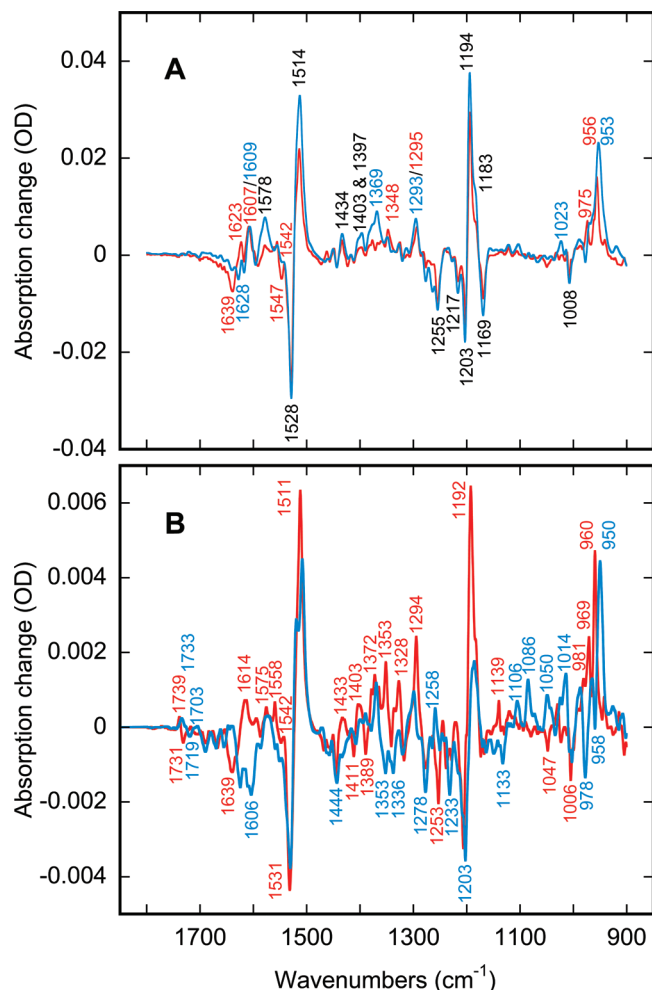
Figure 1. Low-temperature FTIR spectra of bacteriorhodopsin (panel A) and xanthorhodopsin (panel B) in H_2O (red) and D_2O (blue), trapped during blue illumination at 80 K.

in Figure 1A and B, respectively. The spectra in Figure 1A are the well-described low-temperature K spectra of bacteriorhodopsin.[41–43] The similarity between the spectra of bacteriorhodopsin (Figure 1A) and xanthorhodopsin (Figure 1B), and specifically the pattern of the HOOP bands (Figure 2B and D), is extraordinary, and the xanthorhodopsin spectra are more like those of bacteriorhodopsin than most of the other retinal proteins, e.g., halorhodopsin,[52] pharaonis[53,54,59] and Anabena[57] sensory rhodopsins, proteorhodopsin,[55,60] Neurospora rhodopsin,[56,58] and Leptosphaerium rhodopsin.[58]

Besides the similarity of the K spectra in the two proteins (Figure 1A and B), there are distinct differences as well. The first is the higher amplitudes and more structured pattern of the majority of the bands in the 1200–1500 cm^{-1} region, relative to the strongest bands of the difference spectrum in the ethylenic, fingerprint, and HOOP regions. This could be partly due to anisotropy/polarization effects,[73,74] but our main impression is that the spectrum of xanthorhodopsin at 80 K (Figure 1B) reflects much stronger and more numerous bond distortions than the respective spectrum in bacteriorhodopsin (Figure 1A). Detailed studies of this are not possible at this stage because of the lack of an expression system for constructing mutants of xanthorhodopsin, but the possibilities include contributions from the carotenoid, salinixanthin, which acts as an antenna for retinal in xanthorhodopsin.[64] The carotenoid is expected to be disturbed during the early stages of the photocycle, and, if so, will give rise to bands very similar to those of the retinal. The second

difference is in the C=O stretch region: the bilobe feature at 1731/1739 cm^{-1}, which reflects a distortion in the carboxyl COO$^-$ stretch vibration that results in the upshift of the corresponding band. Most probably, it is due to either a decrease in the hydrogen-bonding strength or to a transiently increased proton affinity of the COOH group.[75] In bacteriorhodopsin, a similar but lower amplitude bilobe feature at 1730/1740 reflects an opposite change that leads to the downshift of the COOH$^-$ stretch band. The third difference is the anomalous D_2O-sensitive behavior of the 1253 cm^{-1} band in xanthorhodopsin, unexpected because it is normally attributed to the $C_{12}-C_{13}$ vibration of the retinal.[50] The fourth difference consists of the D_2O-enhanced bands in the 1010–1110 cm^{-1} region, which have never been properly assigned.

Raising the temperature from ~80 to 135 K gives rise to partial conversion from the low-temperature to a higher-temperature K intermediate, which strongly affects the HOOP band region.[15] This process is even more pronounced in xanthorhodopsin, in which, unlike in bacteriorhodopsin,[48] the rise of L does not interfere with the K spectra until above 190 K. Figure 2 presents the spectra of photoequilibrium mixtures created by blue-light illumination at different temperatures. The spectra of bacteriorhodopsin and xanthorhodopsin retain their similarity with increasing temperature (Figures 2 and 3), indicating that a similar secondary K-like intermediate is produced in both proteins upon heating (Figure 2B and D). The greatest changes between the two K-like intermediates are in the HOOP region, which is shown in more detail in Figure 2B and D. Other strong changes (Figure 2A and C) affect the amplitudes of the following features: (i) in the carboxylic region the upshift from 1731 to 1739 cm^{-1} in xanthorhodopsin and the downshift from 1739 to 1730 cm^{-1} in bacteriorhodopsin; (ii) the protonated Schiff base stretch, which is at 1608–1609 cm^{-1} in bacteriorhodopsin,[50,51] and we tentatively assign the analogous band at 1611 cm^{-1} in xanthorhodopsin to the same mode; (iii) the ethylenic band at 1514 in bacteriorhodopsin and at 1511 cm^{-1} in xanthorhodopsin; and (iv) the fingerprint region band at 1194 cm^{-1}. Other notable changes in the two proteins are in the two amide regions: near 1660–1700 and 1560–1580 cm^{-1}. Bands at 1353 and 1389 cm^{-1} in bacteriorhodopsin and xanthorhodopsin, respectively, which are most probably due to the N–H wag,[50] disappear with increasing temperature.

The extended temperature range for xanthorhodopsin where K is the sole product reveals details not immediately evident in bacteriorhodopsin spectra. Specifically, at 190 K, the pattern of the HOOP bands (Figure 2D) becomes virtually indistinguishable from that of the K_E intermediate (see Figure 4 in ref 28), the first of the two K states time-resolved in hundreds of nanoseconds at room temperature. This is less evident in the data for bacteriorhodopsin but is revealed by spectral deconvolution (see below). The agreement of the spectra establishes a correlation between the second K-like state observed here at higher temperature in cryogenic trapping and the time-resolved K_E state observed at room temperature.

Spectral decomposition, performed with the GRAMS software, revealed that the HOOP band region is a superposition of six separate positive bands. These are at 942, 956, 963, 975, 985, and 997 cm^{-1} in bacteriorhodopsin and at 942, 954, 960, 971, 981, and 992 cm^{-1} in xanthorhodopsin, respectively. Figure 3 illustrates this deconvolution for spectra measured in both bacteriorhodopsin and xanthorhodopsin. Figure 4 presents the temperature dependence of the fitted amplitudes for the six HOOP bands in xanthorhodopsin (the analogous data for bacteriorhodopsin are not shown). Only two bands, at 960 and
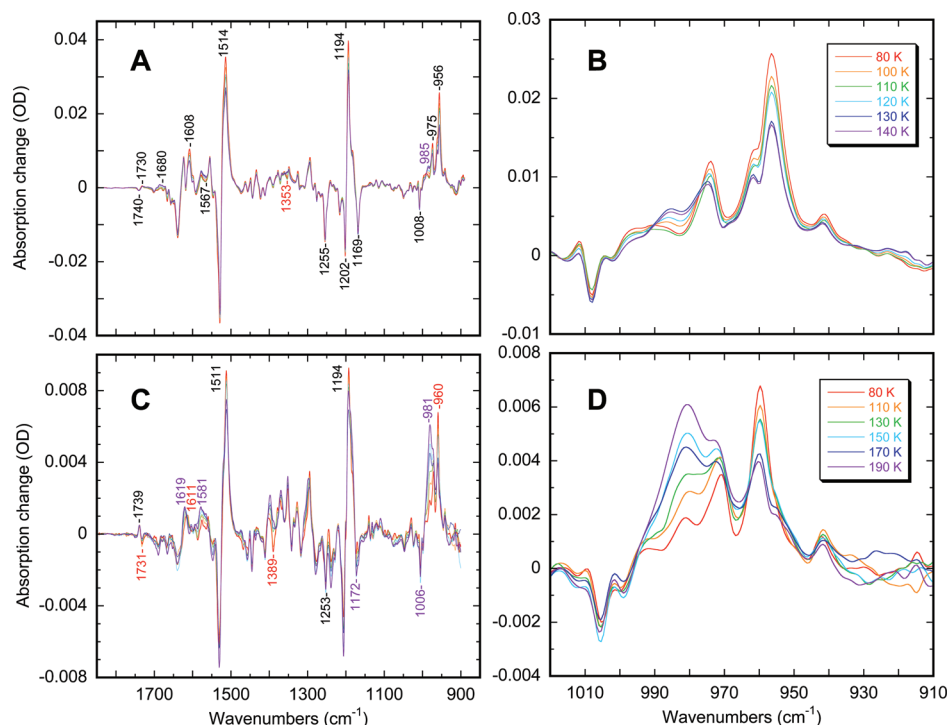
Figure 2. Light-induced mixtures of K states trapped during blue-illumination at different temperatures. In bacteriorhodopsin (panels A and B) and in xanthorhodopsin (panels C and D) at 80 K (red), 100 K (yellow), 110 K (green), 120 K (cyan), 130 K (blue), and 140 K (magenta) for bacteriorhodopsin and at 80 K (red), 110 K (yellow), 130 K (green), 150 K (cyan), 170 K (blue), and 190 K (magenta) for xanthorhodopsin, respectively.
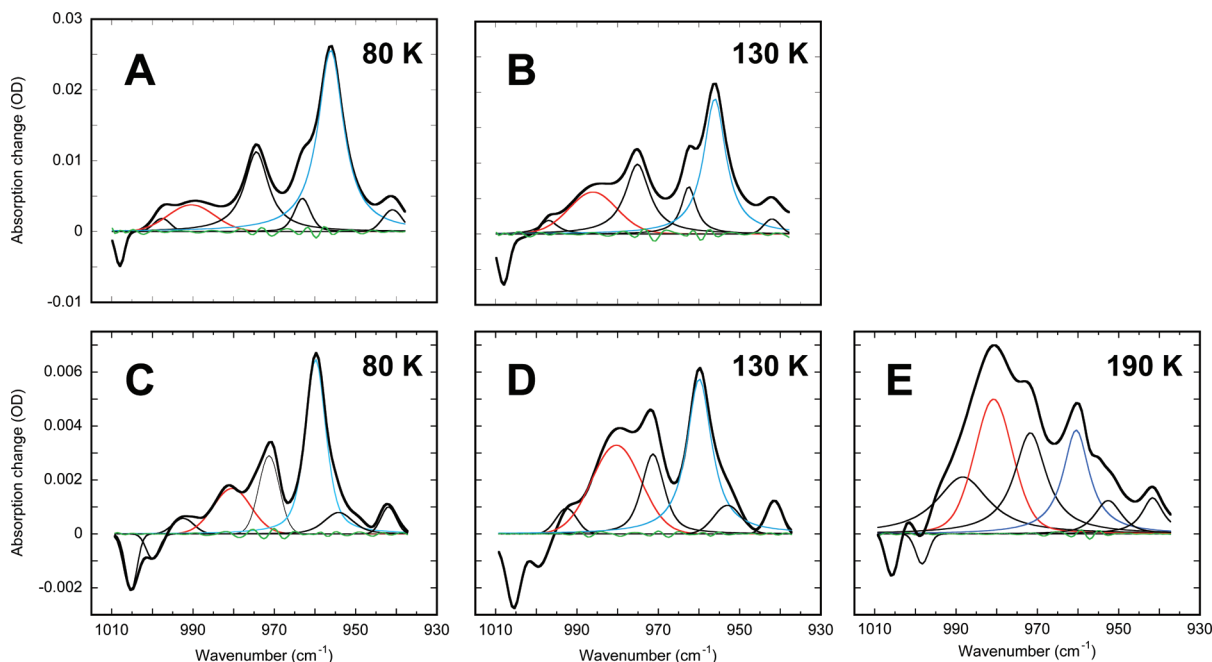

Figure 3. Decomposition of the region of the HOOP bands (from Figure 2) with a weighted sum of Gaussian and Lorentzian components: in bacteriorhodopsin spectra at 80 and 130 K (panels A and B) and in xanthorhodopsin spectra at 80, 130, and 190 K (panels C–E). The deconvolution was done in GRAMS software, yielding fits with r^2 better than 0.997. The fit residuals are plotted in green. In bacteriorhodopsin, the positions (their widths in brackets) for the fitted bands averaged over six temperatures are at 941.6 ± 0.4 cm^{-1} (5.1 ± 0.6), 956.2 ± 0.1 cm^{-1} (6.9 ± 0.5), 962.9 ± 0.4 cm^{-1} (5 ± 1), 974.8 ± 0.3 cm^{-1} (6.6 ± 0.6), 985 ± 2 cm^{-1} (15 ± 1), 997.0 ± 0.3 cm^{-1} (4.7 ± 0.5), and 1008.0 ± 0.1 cm^{-1} (2.8 ± 0.3). In xanthorhodopsin, the corresponding values are 941.5 ± 0.3 cm^{-1} (5.2 ± 0.7), 953.4 ± 0.6 cm^{-1} (7.5 ± 0.8), 960.0 ± 0.2 cm^{-1} (6.8 ± 0.6), 971.5 ± 0.2 cm^{-1} (8 ± 2), 980.5 ± 0.6 cm^{-1} (12 ± 1), 992 ± 2 cm^{-1} (8 ± 2), 999.0 ± 0.7 cm^{-1} (5 ± 1), and 1005.6 ± 0.2 cm^{-1} (4.1 ± 0.3). The two main temperature-sensitive bands are at 956 cm^{-1} (in blue) and 985 cm^{-1} (in red) in bacteriorhodopsin (panels A and B) and at 960 cm^{-1} (in blue) and 981 cm^{-1} (in red) in xanthorhodopsin (panels C–E). Previously, the Raman band at 1008 cm^{-1} in nonexcited BR$_{568}$ was assigned to the symmetric methyl rock, i.e., to the in-plane rather than out-of-plane vibration,[50] implying a similar assignment for the negative band (i.e., depletion in nonexcited state) at 1008 cm^{-1} in bacteriorhodopsin and two similar bands, at ∼1000 and ∼1005 cm^{-1}, in xanthorhodopsin.

981 cm^{-1}, are strongly temperature sensitive (Figure 4), and the pattern of their temperature dependence suggests the

possibility of a temperature-controlled equilibrium between two K-like intermediates.
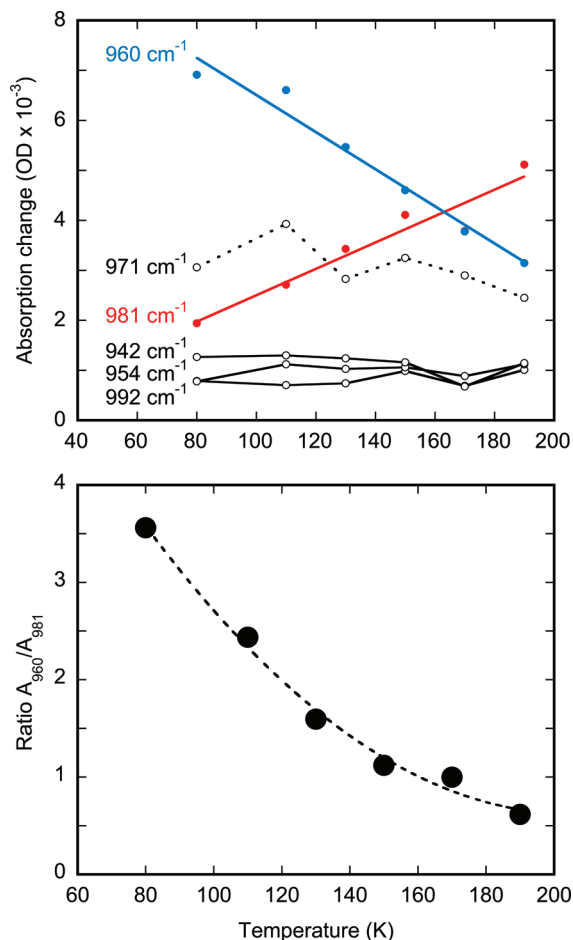
Figure 4. Temperature dependence of the HOOP bands in xanthorhodopsin. Panel A: The amplitude of the decomposed components (as in Figure 3). Panel B: The ratio of amplitudes of the two main temperature-dependent bands A_{960}/A_{981}.
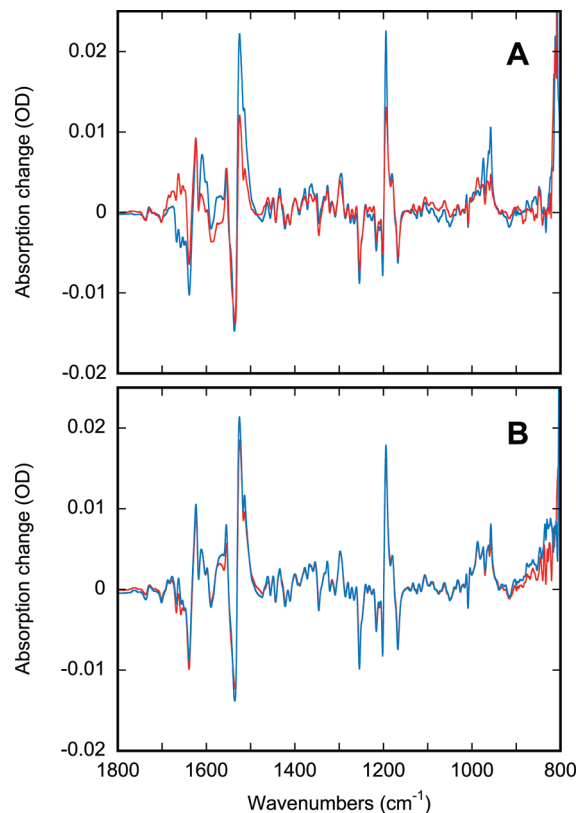

Figure 5. Temperature perturbation experiments with bacteriorhodopsin. Panel A: Effect of upshift of temperature, which illustrates the forward reaction; the light-induced conversion was initiated at 80 K (in blue) and the sample was later heated to 140 K (in red) in the dark. Panel B: Absence of effect from downshift of temperature, which illustrates the absence of the back reaction; the light-induced conversion was initiated at 140 K (in red), and the sample was later cooled to 80 K (in red) in the dark. The shoulder in the ethylenic band reflects incomplete light adaptation, most probably due to insufficient hydration of the sample.

To test this option, we performed temperature-jump experiments, in which the photoequilibrium created at 80 K was heated to 140 K for measurements and the one created at 140 K was cooled to 80 K for measurements. The result is presented in Figure 5, from which it is evident that *upshift* of temperature does lead to the expected shift in the mixture composition while *downshift* fails to affect the composition of the mixture. Thus, the temperature perturbation experiment reveals the absence of the back-reaction, and what looks like an apparent balance in Figure 4 cannot originate from a temperature-controlled equilibrium. The remaining alternative is the distributed kinetics we had found earlier, with a similar approach, for other transitions in bacteriorhodopsin at temperatures below ∼245 K.[48,65]

That distributed kinetics describes the low-temperature transformations between the K-likes states is not a surprise *per se*, since it was observed for both L formation[48] and L decay[65] at still higher temperatures. However, for the L transitions, not only the partial transformation but the characteristic time progression of the distributed kinetics could be observed in real time.[48,65] Here, we were not able to time-resolve the transformation between the K intermediates. It appears that at all temperatures the apparent partial transformation (Figure 4) was accomplished within the illumination period (1−10 min), and the created photoinduced mixture was then stable on the time scale of several hours. This behavior implies that, unlike for the next, K-to-L, transition (for which the underlying barrier-height distribution has a half-maximal width of ∼7 kJ/mol[48]), the energy barrier distribution for transitions between K-like

states must be wide, allowing substantial transformations both on the fast (<1 min) and extremely slow (>200 min) time scales.

The temperature-controlled redistribution pattern of HOOP intensities (Figures 2−4) indicates that the large 981 cm⁻¹ band (in xanthorhodopsin and at 985 cm⁻¹ in bacteriorhodopsin) is specific to the K-like state that dominates at higher temperatures. It is produced from the previous K state at lower temperature (Figure 5A), for which the HOOP band at 961 cm⁻¹ (in xanthorhodopsin and at 956 cm⁻¹ in bacteriorhodopsin) is specific. The temperature dependence (Figure 4 for xanthorhodopsin; analogous data for bacteriorhodopsin are not shown) indicates that neither of the two intermediates is trapped in pure form throughout the entire 80−180 K range, but both are present as temperature- and protein-specific mixtures. This is true even at 77 K, a temperature at which the trapping is widely assumed to produce a single K state.

To obtain the pure spectra of the two K intermediates, the spectra (for bacteriorhodopsin and xanthorhodopsin in Figure 2A and C, respectively) were at first subjected to singular value decomposition (SVD). SVD produced in both cases two statistically significant spectral components, reflecting the presence of two spectrally distinct intermediates. Since the K spectra have many common features (see Figure 2), the first SVD component is effectively a (weighted) sum of the spectra of the two intermediates, while the second component is their difference; both are averaged over all temperatures. A weighted (with singular values) sum and difference of the first two SVD
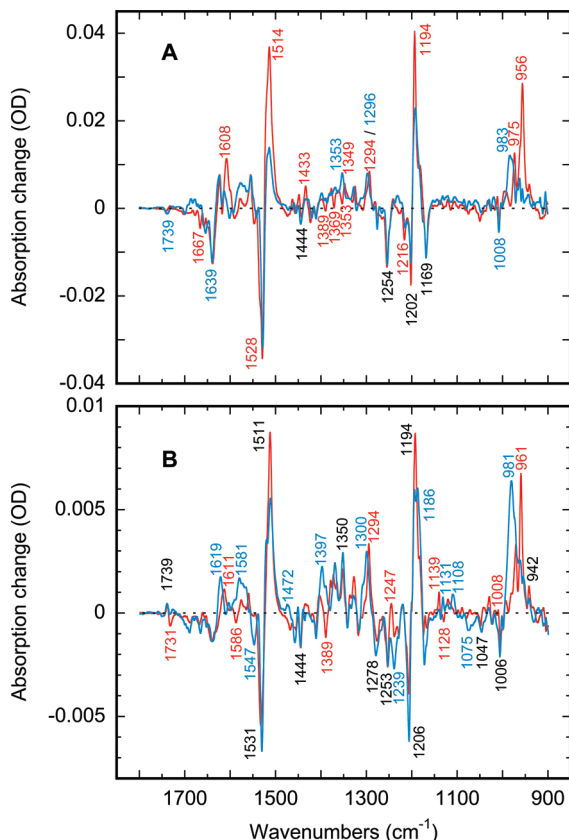
Photocycles of Bacteriorhodopsin and Xanthorhodopsin

J. Phys. Chem. B, Vol. 114, No. 8, 2010 **2925**

Figure 6. Two distinct K intermediates in bacteriorhodopsin (panel A) and xanthorhodopsin (panel B) obtained from the spectra in Figure 2 by decomposition, involving SVD, rotation, and subtraction (see text for details).

components, an orthogonal pair of abstract spectra, were constructed, which represent a starting estimate for the pure spectra of intermediates. These spectra were then rotated, without compromising their orthonormality, with the aim to obtain simultaneously in the *first* spectrum maximum amplitude for the ~960 cm^{-1} band *and* as little as possible (but nonnegative) absorption at ~980 cm^{-1}. This rotation creates the spectrum of the state dominating at low temperatures but already lacking the contribution of the higher-temperature state. Since the real spectra are not orthonormal, the initial rotation leaves significant contribution of the K intermediate that dominates at low temperature, in the *second* spectrum. The latter was eliminated by interactive subtraction. The two calculated spectra were normalized (at 1254 for Figure 6A or 1253 cm^{-1} for Figure 6B), and the result, the spectra that would have been measured for the two pure K-like states in bacteriorhodopsin and in xanthorhodopsin are presented in Figure 6.

Once the measured spectra (in Figure 2) were decomposed into two pure components (in Figure 6), their related contributions, as a function of temperature, could be calculated. In matrix notation, the absorption changes (in Figure 2) measured at different temperatures, $\|\Delta A(v, T)\|$, could be represented as a product of pure spectra of the respective states, $\|\text{spectra}(v, i)\|$, and their temperature-dependent (partial) contributions, $\|\text{contributions}(i, T)\|$:

$$\|\Delta A(v, T)\| = \|\text{spectra}(v, i)\| \cdot \|\text{contributions}(i, T)\| \tag{1}$$

Therefore, a least-squares estimate (averaged over the whole spectrum) for related contributions is readily obtained using the matrix pseudoinverse function:

$$\|\text{contributions}(i, T)\| = \text{pinv}(\|\text{spectra}(v, i)\|) \cdot \|\Delta A(v, T)\| \tag{2}$$

where $\text{pinv}(\|\text{spectra}(v, i)\|) = (\|\text{spectra}(v, i)\|^{\text{T}} \cdot \|\text{spectra}(v, i)\|^{-1} \cdot \|\text{spectra}(v, i)\|^{\text{T}}$ and $\|\ \|^{\text{T}}$ and $(\ )^{-1}$ are the matrix transpose and matrix inverse, respectively. The result is shown in Figure 7. When compared in the same temperature region (80–140 K), the temperature dependences for the composition of the mixtures that are trapped at different temperatures are very similar in both proteins. Extrapolation of these temperature dependences in Figure 7 predicts that the two K intermediates should be expected to coexist in the temperature range from ~50 to ~230 K. This estimate is true for both bacteriorhodopsin and xanthorhodopsin, but this range might differ in other proteins. For example, while it takes temperatures >80 K to observe this transition in both (wild-type) bacteriorhodopsin and xanthorhodopsin, it seems to be nearly completed already at 77 K in Leptosphaerium rhodopsin[58] and in the Y57D mutant of bacteriorhodopsin (see Figure 5 in ref 76) and probably in Salinibacter sensory rhodopsin I (see Figure 2 in ref 63) as well.

The strongest differences between the two K states, in the HOOP region, are evident already in the raw data (Figure 2B and D); other differences were revealed by the spectral decomposition (Figure 6). These differences are similar in the two proteins, but seem more pronounced in xanthorhodopsin. A characteristic change is in the carboxylic region, where a downshift and an upshift of the carbonyl band are present in the low-temperature spectra of bacteriorhodopsin and xanthorhodopsin, respectively (Figures 1 and 6). In xanthorhodopsin, the transition from the low-temperature to the higher-temperature K state affects the bilobe difference carbonyl band at 1739/1730 cm^{-1}, which loses some of the negative (depletion) amplitude without a comparable effect on the positive amplitude. In bacteriorhodopsin, the effect is the opposite, and it is the positive amplitude of the bilobe feature at 1739/1730 cm^{-1} which seems to be primarily affected. Most probably the same explanation applies to both: a second carboxylic acid additionally disturbed in the species that dominates at higher temperatures, although xanthorhodopsin lack a homologue of Asp-115 in bacteriorhodopsin. In both proteins, the protonated Schiff base stretch, at 1608 cm^{-1} in bacteriorhodopsin[42,51] and at 1611 cm^{-1} in xanthorhodopsin, is upshifted to 1625 and 1619 cm^{-1}, respectively. The ethylenic band, at 1514 cm^{-1} in bacteriorhodopsin and 1511 cm^{-1} in xanthorhodopsin, is not significantly affected, implying the absence of a substantial (>5 nm) difference in the visible absorption maxima of the two K intermediates. The depletion band at 1389 cm^{-1} disappears in both proteins at higher temperatures, as a result appearance of an overlapping positive band (at 1397 cm^{-1} in both bacteriorhodopsin and xanthorhodopsin). This band is most probably due to in-plane methyl rock, which spans the 1270–1360 cm^{-1} range in bacteriorhodopsin,[50] or it could reflect the symmetric band of a deprotonated carboxylic acid.[77] An analogous effect is observed in xanthorhodopsin at 1239/1247 cm^{-1} (Figure 6B). The corresponding band is most probably from protonated tyrosine.[77] In bacteriorhodopsin, this effect is much less pronounced but the change in the absorption in the 1210–1250 region is obvious (Figure 6A).

While the differences between the two K-like states observed at cryogenic temperatures is spread throughout the whole mid-
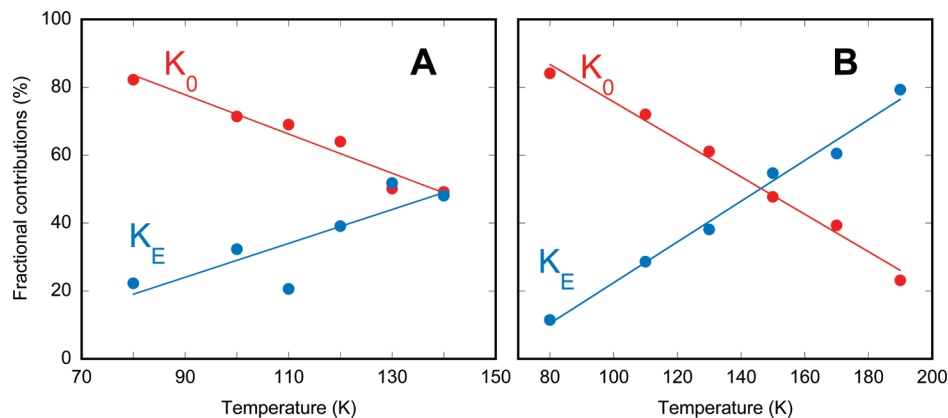
Figure 7. Fractional contributions for the two K states calculated using the deconvoluted spectra of the pure forms (Figure 6) and the raw spectra in Figure 2 (see text for details).
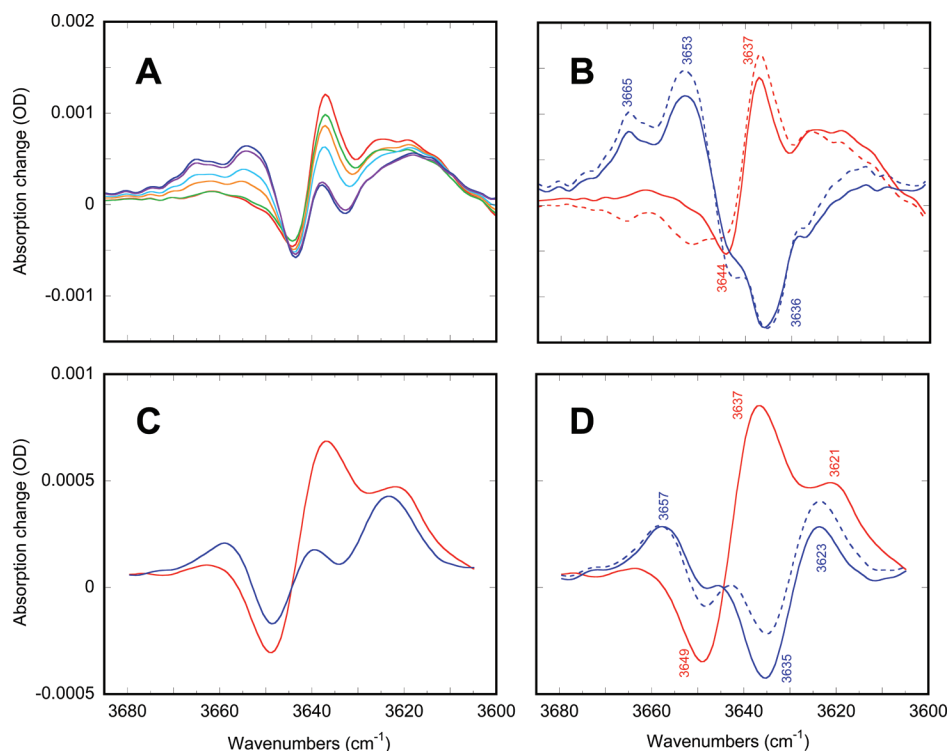

Figure 8. Spectra of the two K-like states in the water region in bacteriorhodopsin (panels A and B) and in xanthorhodopsin (panels C and D). The spectra in panels A and B are at 2 cm^{-1}, as all the rest of the data in this paper; for presentation purposes, the spectra in panels C and D were additionally smoothed to ~3.5 cm^{-1} resolution. Panels A and C are the measured IR spectra (corresponding to the spectra in Figure 2) of mixtures of the two K-like states trapped during blue light illumination at particular temperatures. Panel A: in bacteriorhodopsin at 80 (red), 100 (yellow), 110 (green), 120 (cyan), 130 (blue), and 140 K (magenta). Panel B: in xanthorhodopsin at 85 (red) and 180 K (blue). Panels B and D: Spectral decomposition based on the relative contributions (Figure 7) of the two states calculated from spectra in Figure 6 (dashed lines) and their additional adjustment (solid lines). See text for details.

IR region (Figure 6), the most characteristic changes are in the HOOP region, and the latter primarily influence the calculated ratios of the partial contributions. The ratios (Figure 7) are sensitive to potential errors in spectral deconvolution (in Figure 6), and the strong dependence on one particular feature, the HOOP bands, makes them somewhat unreliable. Therefore, we looked for independent evidence outside the mid-IR region, and explored the O−H stretch region of the free or weakly hydrogen-bonded water (>3600 cm^{-1}) in which differences were previously found between the K-like states trapped at 77 K[78] and at 135 K.[34] Figure 8A and C presents the measured data that reflects a characteristic change in the O−H stretch region in bacteriorhodopsin and xanthorhodopsin, respectively, which is dominated by contributions from one[34] or two (as we think more likely) different weakly hydrogen-bonded water molecules. As

was reported earlier,[78] the main feature in the mixture at 80 K is the downshift of the 3644 cm^{-1} (3649 cm^{-1} in xanthorhodopsin) band to 3637 cm^{-1}, originating from an increased interaction of a water molecule, observed already at the lowest temperature (~80 K). These bands are shifted in D$_2$O and in H$_2$^{18}O,[34,78] and disappear in Y57D mutant.[78] The depletion band at ~3644 cm^{-1} is also present in both L[78,79] and M states.[78]

In contrast, the main apparent feature in the mixture at 140 K seems to be the upshift of a band to ~3653 cm^{-1} (in bacteriorhodopsin and to ~3657 cm^{-1} in xanthorhodopsin), originating from a decreased interaction of either the same water[34] or an O−H stretch, different from that of the water molecule affected at 80 K.

It is important that, in addition to these dominant features at the two extreme temperatures, each of the spectra at 80 and

Photocycles of Bacteriorhodopsin and Xanthorhodopsin

J. Phys. Chem. B, Vol. 114, No. 8, 2010 **2927**

140 K (Figure 8A and C, as well as the other spectra shown for bacteriorhodopsin in the 80−140 K range in Figure 8A) contain weaker additional bands at ∼3637 cm^{-1} at 80 K and the 3644−3649 cm^{-1} band at 140 K. The simultaneous presence of these distortions at both 80 and 140 K could be rationalized by temperature-induced conversion from one state into the other. If the states trapped at both low (at ∼80 K) and high (at ∼140 K) temperatures are (almost) pure states, as was assumed in ref 34, the single depletion band at 3644−3649 cm^{-1} (Figure 8A and C) originates from a single water molecule, and it is the mode of its distortion that is changed upon the temperature-induced conversion from one state into the other. Alternatively, the spectra at the low and high temperatures represent mixtures of two K intermediates, as suggested by our treatment of spectra in the mid-IR region (Figures 6 and 7), and therefore, the change in spectra is due to partial redistribution between those states (at 80 vs at 140 K) that are not present in pure form at either temperature. If there are mixtures of the two states at all temperatures, as we argue, these two states could involve participation of different water molecules, specifically perturbed in one but not in the other state.

To test the spectral deconvolution in Figure 6, we used the partial concentrations calculated from the mid-IR region (Figure 7) to decompose measured spectra in the water region (in Figure 8A and C) into two components, which would reflect the pure spectra of the two K states dominating at low and high temperature, respectively:

$$||\text{spectra}(v, i)|| = ||\Delta A(v, T)|| \cdot \text{pinv}(||\text{contributions}(i, T)||) \quad (3)$$

The results are shown in dashed lines in Figure 8B and D for bacteriorhodopsin and xanthorhodopsin, respectively. Two important features become evident from such deconvolution. The first is that, unlike the raw data (Figure 8A and C), the recalculated spectra (of what we expect to be almost pure states at low and higher temperatures, respectfully) strongly indicate the presence of two distinct depletion bands at 3644/3649 and 3635/3636 cm^{-1} (in bacteriorhodopsin and xanthorhodopsin, respectively). The second feature is that both extrapolated spectra still seem to be partly contaminated by the spectrum of the other state. To estimate the magnitude of this cross-contamination, we interactively subtracted these spectra (dashed lines in Figure 8A and C) from one another with the target to further separate the two tentative depletion bands. The result of this subtraction is shown as solid lines in Figure 8B and D for bacteriorhodopsin and xanthorhodopsin, respectively. To test the validity of this adjustment, the fractional concentrations were then recalculated using eq 2, now based on the spectra (solid lines in Figure 8B and D) from the water region deconvolution. The fractional concentrations (as in Figure 7) were similar to those from the HOOP deconvolution. In xanthorhodopsin, the strongest change is in the calculated fractions at the highest end of temperature data: the mixture composition at 180 K is changed from ∼30:70 to ∼40:60. In bacteriorhodopsin, the effect is on the lowest end of the temperature range, and the corresponding ratios in the mixture composition are changed from ∼80:20 to 85:15. We believe that these differences are within the limit of accuracy of our method, and the separation of the two water bands, with little contamination of one with the other, goes hand-in-hand with the HOOP band separation. Thus, the spectra from the water region confirm that the two K intermediates are trapped as mixtures at both 80 and 140 K.

Separation of the contribution of the two K intermediates in the mixtures trapped at different temperatures resulted in two distinct depletion bands in the water region of both proteins (solid lines in Figure 8B and D), indicating involvement of two different weakly hydrogen-bonded water molecules in the K states. This conclusion is in contradiction with the interpretation in ref 34. Further, each of the two disturbed waters is specific for one of the two K-like states trapped. In both proteins, the water (Figure 8B and D), which has a depletion band (i.e., absorbs in the nonexcited state) at 3644 and 3649 cm^{-1} (in bacteriorhodopsin and xanthorhodopsin, respectively), is the only water disturbed in the K-like state predominant at lower temperatures. The pattern of the distortion of the other water molecule in the two proteins was found to be different (Figure 8B and D) from what it might have looked like in the measured spectra (in Figure 8A and C): its depletion band (i.e., the band of nonexcited bacteriorhodopsin and xanthorhodopsin) is some 10−15 cm^{-1} below the position of the apparent minimum (in Figure 8A and C) and is at 3636/3635 cm^{-1}. This band is present only in the higher temperature K state, which constitutes ∼50% of the mixture at ∼140 K in both proteins, and upon its formation the band is upshifted to 3653 cm^{-1}.

The apparent depletion band at ∼3645 cm^{-1} (first observed in bacteriorhodopsin[78]) was at first tentatively assigned to a water molecule close to Tyr-57[78] and later to water 401[34] in the crystal structure of bacteriorhodopsin.[80] This high frequency implies that it originates from a non-hydrogen-bonded or weakly hydrogen-bonded O−H.[81] If there are two distinct although not greatly different depletion bands, as we observe (Figure 8B), the assignment would have to include water 407 as well, the other water molecule in the vicinity of the Schiff base which also has a non-hydrogen-bonded O−H group and could have an O−H stretch above 3600 cm^{-1}.

In xanthorhodopsin, interpretation of the directly observable depletion band (Figure 8C) in the region of very weakly bound water is much less clear. The crystallographic structure[67] reveals only three water molecules, and only one of them, water 402, in the extracellular region vs. seven in bacteriorhodopsin.[80] This is not likely to be an artifact because the hydrogen bonds that involve water in bacteriorhodopsin are present in xanthorhodopsin also, but they are to main-chain atoms.[67] Water 402 in xanthorodopsin[67] is the analogue of water 402 in bacteriorhodopsin,[80] and, therefore, is a poor candidate for a non-hydrogen-bonded O−H stretch.[67,80] The paucity of other water molecules makes the assignment of the second depletion band in this region, at 3635 cm^{-1}, problematic. This band has to be from a non-hydrogen-bonded O−H stretch.[81] Besides water, −OH groups are in Ser, Thr, Tyr, as well as Asp and Glu, but these seem to be ruled out by the fact that the bands are shifted by H$_2$^{18}O exchange.[34,78]
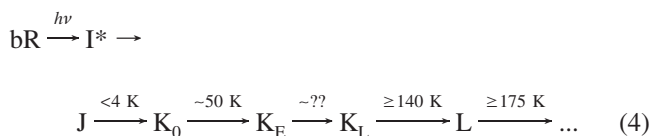
Discussion

As discussed in the Introduction, the need for more than one K intermediate has been recognized for a long time, but the usual option was a second K-like state when one was not sufficient to account for the data.[14−31] The only evidence for more than two distinctly different K states was in ref 19, where the interpretation focused on conformers formed in parallel from an inhomogeneous population of bacteriorhodopsin at cryogenic temperatures. Here, we report on multiple distinct K intermediates. Unlike the three K states in ref 19 (see also ref 34) that differed in their convertibility by visible light of different wavelengths, the two K-like states here (Figure 6) exhibit little if any shift in the ethylenic band, and therefore are expected[82] to have the same visible absorption maximum.

These two K intermediates are formed in sequence in the main path of the photocycle. We do observe them at low temperatures but neither their number nor their sequence is restricted to cryogenic temperatures, and they can be observed at room temperature as well. The two modes of studying the photocycle, low-temperature trapping and time-resolved monitoring, produce complementary results. However, the spectral changes measured reflect complex mixtures rather than pure intermediates in both time-resolved[83–85] and cryogenic trapping[48,62,65] data. Their quantitative comparison is made difficult by the complexity of the deconvolution,[83,84,86] and at least part of the well-documented discrepancies (see, for example, refs 24 and 84) could be due to incomplete separation of the intermediates involved. We believe that multiple distinct K intermediates reported here and previously[16,28] would help to reconcile some of the conflicting data on the early stages of the photocycle.

Interconversions between the K intermediates lead to characteristic changes in the HOOP region (Figure 2B and D), and these states coexist free from contamination from non-K-like states (Figure 2A and C) in a wide temperature rage. In bacteriorhodopsin, this range spans ~60 K, between 77 and ~140 K. In xanthorhodopsin, the temperature-induced variations in spectra are very similar to those in bacteriorhodopsin (Figure 2A and C), and their HOOP regions are practically indistinguishable (when compared in the same temperature region, Figure 2B and D) but the region of coexistence of the two K states uncontaminated by other states (Figure 2B) is increased to span ~110 K, between 77 and ~190 K (Figure 2C).

It was this extended temperature range in xanthorhodopsin (Figure 2C and D) which enabled a more complete conversion and facilitated deconvolution of the two low-temperature K-like states (Figures 3, 4, and 6). The IR spectra (Figure 6B), especially their HOOP region, allowed us to conclude that the K state that dominates at higher temperatures is equivalent to K_E, the *first* of the two K-like states, which were detected in time-resolved measurements at room temperature.[28] Thus, the combination of static low-temperature[15,34] and time-resolved ambient-temperature[24–28] IR spectra provided the initial evidence, but the data from xanthorhodopsin (Figure 6B) and its comparison with the time-resolved spectra[28] and static spectra from bacteriorhodopsin (Figure 6A) has led to the unambiguous conclusion that *there are three distinctly different K intermediates*, and they occur in sequence in the photocycles of the two proteins.

Therefore, based on the results in this paper, and supported by a large body of consistent evidence in the literature (see Introduction), we believe that the initial part of the photocycle is described by the following sequence:

$$bR \xrightarrow{h\nu} I^* \rightarrow$$

$$J \xrightarrow{<4\ K} K_0 \xrightarrow{\sim 50\ K} K_E \xrightarrow{\sim ??} K_L \xrightarrow{\geq 140\ K} L \xrightarrow{\geq 175\ K} ... \quad (4)$$

where the numbers above the arrows indicate the threshold temperatures, i.e., the stability region for the previous intermediate (for bacteriorhodopsin). A similar sequence of K states occurs in the xanthorhodopsin photocycle. The first state that we propose to call K_0 is preferentially trapped at 77–80 K,[41–43] and while it is routinely considered to be the only contribution at this temperature, our estimate is that it accounts for ~85% of K at 77 K. The second one, K_E, was first noted in the mixture trapped at 135 K,[15] in which according to our estimate it

accounts for ~50% of K. K_E is observed as a dominant contribution in room-temperature time-resolved experiments at ~100 ns after excitation.[28] K_L, which is the product of the K_E decay[28] at ambient conditions, cannot be trapped separately from K_E at cryogenic temperatures, due to the slow distributed kinetics and the increasingly faster overlapping formation of L.[48]

In bacteriorhodopsin at ambient conditions, the time constant of J state formation is 430 ± 50 fs;[87] that of the first of the K-like states, K_0, is ~3–5 ps.[13,88] The last of the K states, K_L, decays into L with a time constant of ~1.2 μs.[83] Two additional transitions were reported within the lifetime of the K-like states with time constants of (i) 30–70 ps[23,31,38] and (ii) 50–250 ns,[16,28,32] respectively. We assign the former, with the $\tau_1 = 50 \pm 20$ ps time constant, to the K_0-to-K_E transition; the latter, with the $\tau_2 = 150 \pm 100$ ns time constant, had been already assigned to the K_E-to-K_L transition.[16,28]

The transition from K_0 to K_E results in pronounced rearrangement of bands in the HOOP region. In the K_0 state, the strongest band is at ~956 cm^{-1} (961 cm^{-1} in xanthorhodopsin), which is readily observed when measured either by trapping below ~90 K (Figure 1 and refs 41 and 42) or with a picosecond time resolution.[39] In the K_E state, the strongest band is at ~985 cm^{-1} (Figures 2, 3, and 6), and it is observed in bacteriorhodopsin either as a partial component in a mixture when trapped at 135 K (see Figure 2B and refs 15 and 34), or in a nearly pure form when measured with nanosecond time delay.[28,89] Unlike in bacteriorhodopsin where L formation interferes, in xanthorhodopsin, K_E becomes the major component when trapped at 170–190 K (Figures 2, 3, 4, and 6). Further changes in the HOOP region, which are observed in the ~50 ns to ~0.5 μs range,[24–28] indicate the next process, the decay of K_E into K_L. Unlike the previous transitions, the latter process does not lead to a significant change in the pattern of HOOP band but rather leads to an overall decrease of their amplitude in K_L.[28] Otherwise, K_L has a spectrum[28] that is quite different, particularly in the ethylenic stretch region, from the two previous K-like states, K_0[15,41–43] or K_E.[15,28] Therefore, contrarily to the conclusions in ref 34 (see also ref 58), K_L has little to do with the observed changes between the mixtures trapped at ~80 and at ~135 K.[15,34] Unlike the K-like states, their predecessor, the J state, has either much smaller or no HOOP bands at all,[39] and is not trappable at cryogenic temperatures.[12]

The HOOP bands originate from the wags of the vinyl protons in retinal, from vibrations which are strongly coupled over the double bonds and weakly coupled over the single bonds.[90] There is general agreement that anomalously intense HOOP bands observed in the primary bathoproducts (i.e., K-like states) indicate an unrelaxed torsion distortion of the polyene chain,[90,91] since retinal in solution is planar and does not give rise to HOOP bands (in Raman).[91] There is less agreement about which single or double bonds in the conjugated backbone are distorted and are, therefore, primarily responsible for the HOOP band intensities. The HOOP bands were attributed both to the *single* bond distortions,[24,91,92] i.e., to wags of $C_{10}H-C_{11}H$ with coupling to $C_{12}H$ and of $C_{14}H-C_{15}H$ with coupling to NH, and to torsion distortions of *double* bonds,[90,93] i.e., to $C_7H=C_8H$, $C_{11}H=C_{12}H$, and $C_{15}H=NH$.

The main assignments of the HOOP bands in the microbial rhodopsins were made by Raman spectroscopy for the K state of bacteriorhodopsin, which at 5 cm^{-1} resolution[35] detected four bands[36,50] relevant to our study, at 943, 958, and 975 plus at 1348 cm^{-1}. The 975 cm^{-1} band was assigned to the wags of the C_7-H and C_8-H (i.e., coupled in-phase vibrations of the vinyl protons in $-HC_7=C_8H-$); the 943 cm^{-1} band to the wags

Photocycles of Bacteriorhodopsin and Xanthorhodopsin

J. Phys. Chem. B, Vol. 114, No. 8, 2010 **2929**

of C_{11}—H and C_{12}—H (coupled in-phase in —HC_{11}=$C_{12}H$—), while the 958 cm^{-1} band to the isolated wag of C_{15}—H coupled to the N—H wag at 1348 cm^{-1}. The corresponding out-of-phase vibrations are at 823 and 868 cm^{-1} for the C_7—H/C_8—H and C_{11}—H/C_{12}—H, while the bands for the C_{14}—H and C_{10}—H wags, which are separated from a neighboring C—H by an uncoupling single bond, are at 812 and 899 cm^{-1}, respectively, i.e., all below 900 cm^{-1} (see more in ref 50).

Thus, in the crucial region of 945−995 cm^{-1}, Raman assignments are available for only three bands, at 943, 958, and 975 cm^{-1}, while deconvolution of the IR data produces six positive bands for K-like states: at 942, 956, 963, 975, 985, and 997 in bacteriorhodopsin (Figure 2B) and at 942, 954, 960, 971, 981, and 992 cm^{-1} (Figures 2D and 3) in xanthorhodopsin. The fourth band at ~985 cm^{-1}, which we assign exclusively to K_E, is not expected to be strong and is not seen at 77 K in Raman[36,94] but was observed, in accord with our expectations, at room temperature in nanosecond time-resolved CARS[32] and Raman[22] at 984 and 987 cm^{-1}, respectively. The last two bands at 963 and 997 cm^{-1} in bacteriorhodopsin and at 954 and 992 cm^{-1} in xanthorhodopsin are present in both K_0 and K_E states and exhibit no temperature dependence (Figure 4A). Thus, of the two most interesting bands (Figure 4), at ~960 cm^{-1} (at 956 cm^{-1} in bacteriorhodopsin and at 961 cm^{-1} in xanthorhodopsin), which we assigned exclusively to K_0 (Figure 6A), and at ~980 cm^{-1} (at 985 cm^{-1} in bacteriorhodopsin and at 981 cm^{-1} in xanthorhodopsin), which we assigned exclusively to K_E (Figure 6A), the latter received no clear assignment. The former one, at ~960 cm^{-1}, is known to be[42] the one significantly affected by H_2O/D_2O exchange (see also Figure 1), and its assignment to the 15-HOOP mode (coupled through the double bond to the N—H/D HOOP) has never been challenged.

However, when an assignment was made for the band at ~980 cm^{-1} from FTIR data,[24] it yielded a seemingly paradoxical conclusion that it *also* (as the band at ~960 cm^{-1}) belongs to the 15-HOOP mode. The HOOP band frequencies do not display significant temperature dependence. For example, the strongest band in low-temperature static spectra in bacteriorhodopsin is at 956 cm^{-1},[15,42] and at ~960 cm^{-1} in room-temperature picosecond spectra,[32,39] and, therefore, the increasing amplitude at ~980 cm^{-1} in the trapped mixture at higher temperatures (Figure 4) can hardly be explained as an upshift of its frequency (from ~960 to ~980 cm^{-1}) by temperature-induced factors. Thus, if the band at ~980 cm^{-1} reflects the same mode as the ~960 cm^{-1} band, i.e., 15-HOOP, its increasing amplitude has to be due to the increasing presence of a different intermediate in mixtures trapped at higher temperatures. Therefore, the simultaneous HOOP intensities at ~960 and ~980 cm^{-1} (in the whole 80−180 K range in Figure 4) is direct evidence that the trapped states not only at 140 and 180 K but also at 77 K are not pure states but are mixtures of K_0 and K_E, each contributing its own 15-HOOP mode, at ~960 cm^{-1} an at ~980 cm^{-1}, respectively.

Alternatively, the mode that gives rise to the increasing band at ~980 cm^{-1} at higher temperatures (Figure 3) is not from the 15-HOOP but rather the vibration that contributes to the Raman band at 975 cm^{-1} (obtained with a 5 cm^{-1} resolution), which was assigned to the coupled 7,8-HOOP, i.e., wags of the C_7—H and C_8—H (coupled in-phase —HC_7=C_8H—).[50] If so, the evolution of the HOOP pattern upon heating between 80 and 140 K in bacteriorhodopsin and to ~180 K in xanthorhodopsin provides an interesting possibility, as follows. In the K_0 state, the —C_7=C_8— bonds are virtually undisturbed (absence of a band at ~980 cm^{-1} in Figure 6) in contrast to the strongly

distorted =C_{14}—C_{15}= bonds (the intense band at ~960 cm^{-1} in Figure 6), and the torsional distortion at this early stage is localized close to the Schiff base end of the polyene chain with little if any torsional distortions close to the ionone ring. This pattern is reversed upon the K_0-to-K_E transition (Figure 4), and in the K_E state the strongest distortion is in the —C_7=C_8— region, close to the ionone ring, while the —C_{15}=N— region seems to be relaxed. This relaxation (although only partial, due to distributed kinetics) takes place in bacteriorhodopsin within minutes at temperatures as low as ~140 K (~50% conversion) or even as low as ~80 K (~20% conversion). The distortion in the —C_7=C_8— region (the band at ~980 cm^{-1}) relaxes later, in two stages during the K_E-to-K_L and the K_L-to-L transitions, observable at ambient temperature on the time-scale of ~100 ns[28] and 1.2 μs,[28] respectively.

Both X-ray crystallography[95] and solid-state NMR[92] of the K state at cryogenic temperatures (predominantly K_0, see Figure 7) reveal major torsional distortions near the site of isomerization in the retinal. Thus, the structure of the retinal in K_0 represents a distorted 13-*cis* isomer, which relaxes into planar 13-*cis* isomer in L[96] during the K_0-to-K_E-to-K_L-to-L transitions, as witnessed by the HOOP band relaxation.[28,85] It is not clear at this point which of the three steps, the K_0-to-K_E, the K_E-to-K_L, or the K_L-to-L (in tens of picoseconds,[38] in hundreds of nanoseconds,[28] or in microseconds,[28] respectively), is responsible for most of the relaxation. In bacteriorhodopsin, neither K_E nor K_L can be easily trapped for crystallographic structure determination due to interference from L, which begins to appear above ~140 K.[48] The extended temperature range in xanthorhodopsin, in which the K-like states coexist without interference from L (Figure 2), makes it possible to study the K_0-to-K_E reaction in more detail.

Some residual HOOP bands (~15% intensity) could be found in time-resolved spectra of L as well,[28,85] which allows alternative interpretations. On the one hand, it is possible that the HOOP intensities are characteristic not only for the K-like states but for the L state as well, and, therefore, the retinal is still somewhat twisted in L. The crystallographic data on L does not show sufficient torsional distortions,[96] and the Raman spectra produce no prominent HOOP bands.[50] On the other hand, it is much more probable that the residual HOOP intensity is due to the incomplete deconvolution of the K_L and L kinetics when the back-reaction, K_L ← L,[97–99] was not properly taken into account.[28] Then, the anomalously intense HOOP bands are a unique characteristic feature of the (red-shifted) intermediates, K-like[15,24,28,42] and O-like,[61] formed immediately after isomerization, which have not yet had a chance to relax their torsion stress. We favor this latter interpretation.

Conclusions

Three K-like states, K_0, K_E, and K_L, occur in a sequence in the photocycles of both bacteriorhodopsin and xanthorhodopsin. In IR, these states are distinguished primarily in the HOOP (K_0 vs K_E) and ethylenic (K_E vs K_L)[28] regions. Contrarily to widely held belief, trapping even at 77 K does not result in a single intermediate. Rather, the K_0 and K_E states coexist in the temperature range from ~50 to ~230 K as binary mixtures (plus the L state above 140 K in bacteriorhodopsin and above 190 K in xanthorhodopsin). When trapped at 77 K, the contribution of K_E is ~15 and ~10% in bacteriorhodopsin and xanthorhodopsin, respectively.

Interconversion of K_0-to-K_E is unidirectional, proceeding with a distributed kinetics that is characterized by a barrier-height distribution wider than the ~7 kJ/mol, measured previously for a later reaction, the L-formation.[48]

Two different, rather than one,[34] weakly bound water molecules are disturbed in both proteins during the life span of the K-like states: one in K_0, the other in K_E. In bacteriorhodopsin, the first was assigned to water 401,[34] and the other might have been assigned to water 407. Unlike bacteriorhodopsin, xanthorhodopsin lacks these weakly bound water molecules,[67] presenting a challenge to the interpretation of the observed distortions of weakly bound water molecules.

References and Notes

(1) Béjà, O.; Spudich, E. N.; Spudich, J. L.; Leclerc, M.; DeLong, E. F. *Nature* **2001**, *411*, 786–789.

(2) Wang, W. W.; Sineshchekov, O. A.; Spudich, E. N.; Spudich, J. L. *J. Biol. Chem.* **2003**, *278*, 33985–33991.

(3) Sabehi, G.; Massana, R.; Bielawski, J. P.; Rosenberg, M.; DeLong, E. F.; Beja, O. *Environ. Microbiol.* **2003**, *5*, 842–849.

(4) Brown, L. S. *Photochem. Photobiol. Sci.* **2004**, *3*, 555–565.

(5) Lanyi, J. K. *Annu. Rev. Physiol.* **2004**, *66*, 665–688.

(6) Hoff, W. D.; Jung, K. H.; Spudich, J. L. *Annu. Rev. Biophys. Biomol. Struct.* **1997**, *26*, 223–258.

(7) Lozier, R. H.; Bogomolni, R. A.; Stoeckenius, W. *Biophys. J.* **1975**, *15*, 955–962.

(8) Dinur, U.; Honig, B.; Ottolenghi, M. *Photochem. Photobiol.* **1981**, *33*, 523–527.

(9) Stoeckenius, W.; Lozier, R. H. *J. Supramol. Struct.* **1974**, *2*, 769–774.

(10) Litvin, F. F.; Balashov, S. P.; Sineshchekov, V. A. *Bioorg. Khim.* **1975**, *1*, 1767–1777.

(11) Applebury, M. L.; Peters, K. S.; Rentzepis, P. M. *Biophys. J.* **1978**, *23*, 375–382.

(12) Iwasa, T.; Tokunaga, F.; Yoshizawa, T. *FEBS Lett.* **1979**, *101*, 121–124.

(13) Polland, H. J.; Franz, M. A.; Kaiser, W.; Kölling, E.; Oesterhelt, D.; Zinth, W. *Biophys. J.* **1986**, *49*, 651–662.

(14) Shichida, Y.; Matuoka, S.; Hidaka, Y.; Yoshizawa, T. *Biochim. Biophys. Acta* **1983**, *723*, 240–246.

(15) Rothschild, K. J.; Roepe, P. D.; Gillespie, J. *Biochim. Biophys. Acta* **1985**, *808*, 140–148.

(16) Dioumaev, A. K.; Lanyi, J. K. *J. Phys. Chem. B,* **2009**, *113*, 16643–16653.

(17) Mao, B. *Photochem. Photobiol.* **1981**, *33*, 407–411.

(18) Kalisky, O.; Ottolenghi, M. *Photochem. Photobiol.* **1982**, *35*, 109–115.

(19) Balashov, S. P.; Karneeva, N. V.; Litvin, F. F. *Biol. Membr.* **1990**, *7*, 586–592.

(20) Balashov, S. P.; Karneyeva, N. V.; Litvin, F. F.; Ebrey, T. G. *Photochem. Photobiol.* **1991**, *54*, 949–953.

(21) Kuschmitz, D.; Hess, B. *FEBS Lett.* **1982**, *138*, 137–140.

(22) Braiman, M. S. *Methods Enzymol.* **1986**, *127*, 587–597.

(23) Diller, R.; Iannone, M.; Cowen, B. R.; Maiti, S.; Bogomolni, R. A.; Hochstrasser, R. M. *Biochemistry* **1992**, *31*, 5567–5572.

(24) Weidlich, O.; Siebert, F. *Appl. Spectrosc.* **1993**, *47*, 1394–1400.

(25) Sasaki, J.; Maeda, A.; Kato, C.; Hamaguchi, H. *Biochemistry* **1993**, *32*, 867–871.

(26) Sasaki, J.; Yuzawa, T.; Kandori, H.; Maeda, A.; Hamaguchi, H. *Biophys. J.* **1995**, *68*, 2073–2080.

(27) Hage, W.; Kim, M.; Frei, H.; Mathies, R. A. *J. Phys. Chem.* **1996**, *100*, 16026–16033.

(28) Dioumaev, A. K.; Braiman, M. S. *J. Phys. Chem. B* **1997**, *101*, 1655–1662.

(29) Hsieh, C.-L.; Nagumo, N.; Nicol, M.; El-Sayed, M. A. *J. Phys. Chem.* **1981**, *85*, 2714–2717.

(30) Hsieh, C.-L.; El-Sayed, M. A.; Nicol, M.; Nagumo, M.; Lee, J.-H. *Photochem. Photobiol.* **1983**, *38*, 83–94.

(31) Mizuno, M.; Shibata, M.; Yamada, J.; Kandori, H.; Mizutani, Y. *J. Phys. Chem. B* **2009**, *113*, 12121–12128.

(32) Weidlich, O.; Ujj, L.; Jager, F.; Atkinson, G. H. *Biophys. J.* **1997**, *72*, 2329–2341.

(33) Dioumaev, A. K.; Keszthelyi, L. *Acta Biochim. Biophys. Hung.* **1988**, *23*, 271–278.

(34) Maeda, A.; Verhoeven, M. A.; Lugtenburg, J.; Gennis, R. B.; Balashov, S. P.; Ebrey, T. G. *J. Phys. Chem. B* **2004**, *108*, 1096–1101.

(35) Braiman, M. S.; Mathies, R. A. *Proc. Natl. Acad. Sci. U.S.A.* **1982**, *79*, 403–407.

(36) Smith, S. O.; Braiman, M. S.; Mathies, R. A. *Time-resolved vibrational spectroscopy*; Academic Press: New York, 1983; pp 219–230.

(37) Brack, T. L.; Atkinson, G. H. *J. Mol. Struct.* **1989**, *214*, 289–303.

(38) Doig, S. J.; Reid, P. J.; Mathies, R. A. *J. Phys. Chem.* **1991**, *95*, 6372–6379.

(39) Shim, S.; Dasgupta, J.; Mathies, R. A. *J. Am. Chem. Soc.* **2009**, *131*, 7592–7597.

(40) Terentis, A. C.; Ujj, L.; Abramczyk, H.; Atkinson, G. H. *Chem. Phys.* **2005**, *313*, 51–62.

(41) Rothschild, K. J.; Marrero, H. *Proc. Natl. Acad. Sci. U.S.A.* **1982**, *79*, 4045–4049.

(42) Bagley, K.; Dollinger, G.; Eisenstein, L.; Singh, A. K.; Zimányi, L. *Proc. Natl. Acad. Sci. U.S.A.* **1982**, *79*, 4972–4976.

(43) Siebert, F.; Mäntele, W. *Eur. J. Biochem.* **1983**, *130*, 565–573.

(44) Gerwert, K.; Siebert, F. *EMBO J.* **1986**, *5*, 805–811.

(45) Diller, R.; Maiti, S.; Walker, G. C.; Cowen, B. R.; Pippenger, R. S.; Bogomolni, R. A.; Hochstrasser, R. M. *Chem. Phys. Lett.* **1995**, *241*, 109–115.

(46) Maeda, A.; Sasaki, J.; Pfefferlé, J.-M.; Shichida, Y.; Yoshizawa, T. *Photochem. Photobiol.* **1991**, *54*, 911–921.

(47) Kandori, H. *Biochim. Biophys. Acta* **2000**, *1460*, 177–191.

(48) Dioumaev, A. K.; Lanyi, J. K. *Proc. Natl. Acad. Sci. U.S.A.* **2007**, *104*, 9621–9626.

(49) Smith, S. O.; Lugtenburg, J.; Mathies, R. A. *J. Membr. Biol.* **1985**, *85*, 95–109.

(50) Smith, S. O. Resonance Raman studies on the mechanism of proton translocation by bacteriorhodopsin's retianl chromophore. Ph.D. thesis, University of California, Berkeley, 1985.

(51) Rothschild, K. J.; Roepe, P. D.; Lugtenburg, J.; Pardoen, J. A. *Biochemistry* **1984**, *23*, 6103–6109.

(52) Dioumaev, A. K.; Braiman, M. S. *Photochem. Photobiol.* **1997**, *66*, 755–763.

(53) Kandori, H.; Shimono, K.; Sudo, Y.; Iwamoto, M.; Shichida, Y.; Kamo, N. *Biochemistry* **2001**, *40*, 9238–9246.

(54) Shimono, K.; Furutani, Y.; Kandori, H.; Kamo, N. *Biochemistry* **2002**, *41*, 6504–6509.

(55) Bergo, V.; Amsden, J. J.; Spudich, E. N.; Spudich, J. L.; Rothschild, K. J. *Biochemistry* **2004**, *43*, 9075–9083.

(56) Furutani, Y.; Bezerra, A. G., Jr.; Waschuk, S.; Sumii, M.; Brown, L. S.; Kandori, H. *Biochemistry* **2004**, *43*, 9636–9646.

(57) Furutani, Y.; Kawanabe, A.; Jung, K. H.; Kandori, H. *Biochemistry* **2005**, *44*, 12287–12296.

(58) Furutani, Y.; Sumii, M.; Fan, Y.; Shi, L. C.; Waschuk, S. A.; Brown, L. S.; Kandori, H. *Biochemistry* **2006**, *45*, 15349–15358.

(59) Furutani, Y.; Sudo, Y.; Wada, A.; Ito, M.; Shimono, K.; Kamo, N.; Kandori, H. *Biochemistry* **2006**, *45*, 11836–11843.

(60) Ikeda, D.; Furutani, Y.; Kandori, H. *Biochemistry* **2007**, *46*, 5365–5373.

(61) Smith, S. O.; Pardoen, J. A.; Lugtenburg, J.; Curry, B.; Mathies, R. A. *Biochemistry* **1983**, *22*, 6141–6148.

(62) Maeda, A. *Isr. J.Chem.* **1995**, *35*, 387–400.

(63) Suzuki, D.; Sudo, Y.; Furutani, Y.; Takahashi, H.; Homma, M.; Kandori, H. *Biochemistry* **2008**, *47*, 12750–12759.

(64) Balashov, S. P.; Imasheva, E. S.; Boichenko, V. A.; Anton, J.; Wang, J. M.; Lanyi, J. K. *Science* **2005**, *309*, 2061–2064.

(65) Dioumaev, A. K.; Lanyi, J. K. *Biochemistry* **2008**, *47*, 11125–11133.

(66) Oesterhelt, D.; Stoeckenius, W. *Methods Enzymol.* **1974**, *31*, 667–678.

(67) Luecke, H.; Schobert, B.; Stagno, J.; Imasheva, E. S.; Wang, J. M.; Balashov, S. P.; Lanyi, J. K. *Proc. Natl. Acad. Sci. U.S.A.* **2008**, *105*, 16561–16565.

(68) Dioumaev, A. K.; Lanyi, J. K. *Photochem. Photobiol.* **2009**, *85*, 598–608.

(69) Golub, G. H.; Van Loan, C. F. *Matrix computations*; Johns Hopkins University Press: Baltimore, MD, 1996; 1–694.

(70) Korenstein, R.; Hess, B. *FEBS Lett.* **1977**, *82*, 7–11.

(71) Roepe, P. D.; Ahl, P. L.; Herzfeld, J.; Lugtenburg, J.; Rothschild, K. J. *J. Biol. Chem.* **1988**, *263*, 5110–5117.

(72) Mizuide, N.; Shibata, M.; Friedman, N.; Sheves, M.; Belenky, M.; Herzfeld, J.; Kandori, H. *Biochemistry* **2006**, *45*, 10674–10681.

(73) Earnest, T. N.; Roepe, P. D.; Braiman, M. S.; Gillespie, J.; Rothschild, K. J. *Biochemistry* **1986**, *25*, 7793–7798.

(74) Kandori, H.; Kinoshita, N.; Shichida, Y.; Maeda, A. *J. Phys. Chem. B* **1998**, *102*, 7899–7905.

(75) Dioumaev, A. K. *Biochemistry (Moscow)* **2001**, *66*, 1269–1276.

(76) Sonar, S.; Marti, T.; Rath, P.; Fischer, W.; Coleman, M.; Nilsson, A.; Khorana, H. G.; Rothschild, K. J. *J. Biol. Chem.* **1994**, *269*, 28851–28858.

(77) Barth, A. *Biochim. Biophys. Acta* **2007**, *1767*, 1073–1101.

Photocycles of Bacteriorhodopsin and Xanthorhodopsin

J. Phys. Chem. B, Vol. 114, No. 8, 2010 **2931**

(78) Fischer, W. B.; Sonar, S.; Marti, T.; Khorana, H. G.; Rothschild, K. J. *Biochemistry* **1994**, *33*, 12757–12762.

(79) Maeda, A.; Sasaki, J.; Ohkita, Y. J.; Simpson, M.; Herzfeld, J. *Biochemistry* **1992**, *31*, 12543–12545.

(80) Luecke, H.; Schobert, B.; Richter, H.-T.; Cartailler, J. P.; Lanyi, J. K. *J. Mol. Biol.* **1999**, *291*, 899–911.

(81) Bellamy, L. J. *The infra-red spectra of complex molecules*, 3rd ed.; Chapman and Hall - Wiley: London, New York, 1975; 1−433.

(82) Aton, B.; Doukas, A. G.; Callender, R. H.; Becher, B.; Ebrey, T. G. *Biochemistry* **1977**, *16*, 2995–2999.

(83) Xie, A. H.; Nagle, J. F.; Lozier, R. H. *Biophys. J.* **1987**, *51*, 627–635.

(84) Hessling, B.; Souvignier, G.; Gerwert, K. *Biophys. J.* **1993**, *65*, 1929–1941.

(85) Rödig, C.; Chizhov, I.; Weidlich, O.; Siebert, F. *Biophys. J.* **1999**, *76*, 2687–2701.

(86) Dioumaev, A. K. *Biophys. Chem.* **1997**, *67*, 1–25.

(87) Nuss, M. C.; Zinth, W.; Kaiser, W.; Kolling, E.; Oesterhelt, D. *Chem. Phys. Lett.* **1985**, *117*, 1–7.

(88) Sharkov, A. V.; Pakulev, A. V.; Chekalin, S. V.; Matveetz, Y. A. *Biochim. Biophys. Acta* **1985**, *808*, 94–102.

(89) Kaminaka, S.; Mathies, R. A. *Laser Chem.* **1999**, *19*, 165–168.

(90) Eyring, G.; Curry, B.; Broek, A.; Lugtenburg, J.; Mathies, R. *Biochemistry* **1982**, *21*, 384–393.

(91) Eyring, G.; Curry, B.; Mathies, R.; Fransen, R.; Palings, I.; Lugtenburg, J. *Biochemistry* **1980**, *19*, 2410–2418.

(92) Mak-Jurkauskas, M. L.; Bajaj, V. S.; Hornstein, M. K.; Belenky, M.; Griffin, R. G.; Herzfeld, J. *Proc. Natl. Acad. Sci. U.S.A.* **2008**, *105*, 883–888.

(93) Koyama, Y. *Carotenoids*; Birkhaeuser Verlag: Basel, Switzerland, 1995; Chapter 5, pp 135−146.

(94) Smith, S. O.; Myers, A. B.; Mathies, R. A.; Pardoen, J. A.; Winkel, C.; van den Berg, E. M. M.; Lugtenburg, J. *Biophys. J.* **1985**, *47*, 653–664.

(95) Schobert, B.; Cupp-Vickery, J.; Hornak, V.; Smith, S. O.; Lanyi, J. K. *J. Mol. Biol.* **2002**, *321*, 715–726.

(96) Lanyi, J. K.; Schobert, B. *J. Mol. Biol.* **2007**, *365*, 1379–1392.

(97) Zimányi, L.; Keszthelyi, L.; Lanyi, J. K. *Biochemistry* **1989**, *28*, 5165–5172.

(98) Zimányi, L.; Lanyi, J. K. *Biophys. J.* **1993**, *64*, 240–251.

(99) Zimányi, L.; Saltiel, J.; Brown, L. S.; Lanyi, J. K. *J. Phys. Chem. A* **2006**, *110*, 2318–2321.